Journal of
Engineering Sciences
Faculty of Engineering
Assiut University
JES
مجلة
العلوم الهندسية
كلية الهندسة
جامعة أسيوط
journal homepage: http://jesaun.journals.ekb.eg

Elastic Shear Buckling of Tapered Steel Plate Girders with Opening in Web

Received 28 November 2022; Revised 10 February 2023; Accepted 17 February 2023

Asmaa Y Hamed [1]

Keywords
Critical Shear buckling; Tapered web girder; Circular hole; Square hole; Finite Element; Analytical Analysis

Abstract

Tapered Plate girders are considered the best efficient choice in design of the industrial buildings and bridges with large-span. Openings in the web of plate girders are frequently required to give space for services, resulting in increased fabrication costs and a reduction in load-carrying capability. The aim of the present paper is to estimate the critical shear buckling of tapered plate girders containing a circular or square opening. Finite element simulations were performed on 176 steel beams with prismatic and tapered web containing two different shapes of openings (circular and square). The analysis considered the effects of tapering angle, hole size with respect to the average height of the web, aspect ratio, depth to thickness ratio and the boundary conditions between the web and flanges. The numerical results are used to estimate an analytical expression for the critical shear stress of prismatic and tapered web panels containing a circular or square opening.

1. Introduction

Construction with large scale spans such as Continuous bridges and industrial buildings, plate girders are typically constructed as carried heavy loads (high bending moment and shear forces). So, using tapered shape with variable inertia allows for good stress distribution within the web panel and contributes to wight of steel reduction and decreases the overall structure's cost. On the other hand, opening in plate girder are used for their advantage of allowing essential services as ducts and pipelines. Usually, in modern construction, are needed to apply the two solutions in steel web girders. The shape of the web opening depends on the designer's choice and the purpose of the opening. The depth of these openings is sometimes up to 50% of the beam depth. This type of structure reduces floor height, more systematic plumbing, and duct installation and reduces cost, but it also reduces beam shear strength. Over the past 30 years, extensive research on steel plate structures such as plate box girders and marine double bottoms has led to a better understanding of the behavior and suggested design approaches for these structures with web openings. In 1971, the

[1] Assist. Prof., Structural Engineering Department, the High Institute of Engineering and Technology Luxor, Egypt
asmaa_yasseen@yahoo.com, dr_asmaa11@adj.aast.edu

https://doi.org/10.21608/JESAUN.2023.177464.1184

first study of relevance to thin opening webs was by Hoglund [1] who presented an experimental test on girders containing circular and rectangular web openings. That is found that holes located in the high shear zone resulted in significantly lower loads compared to the girders with openings in the zone of high bending and low shear. Narayanan et.al [2-10] present several studies with detailed information on the behavior of prismatic plate girders with web openings based on which an approximate approach to predict the ultimate capacity of such girders with a cut-out in the web. An equilibrium method in [4-6] is assuming that the width of the membrane stresses developed along the diagonal tension field is reduced by the increase of the dimension of the holes. Also, Narayanan and Avanessian [7] was shown that the holes located in the corner of the web far away as possible from the tension field do not reduce the shear capacity of the girder. In addition, Narayanan, and Avanessian [8] used modified elastic shear stress in the equilibrium solution. By using the virtual working method. And, they provide an expression for estimating the bearing capacity of plate girders with eccentric web holes in their Refs [9-10]. Carlo et al. [11] studied the linear buckling and nonlinear behavior of steel plates under shear loading, considering the effects of size, position relative to the two principal axes, shape (circular or rectangular), and orientation of holes. Regarding the slenderness and aspect ratio of the panel, results for plate girders with web openings shown in Refs [11-16] estimated design concepts for composite structures and other thin-walled components, showing that the presence of web openings results in a loss of strength due to lack of resistance in the web out-of-plane deformation. The ultimate shear strength of perforated web under shear loading was investigated by Paik [17], considering only that the plates simply support all 4-edges and circular cut-out shape, placed in the centre of the panel. Based on the elastic shear buckling of the plate without cut-out given by Timoshenko and Gere [18] Eq. [1].

$$\tau_E = K\frac{\pi^2 E}{12(1-\nu^2)}\left(\frac{t_w}{h_w}\right)^2 \quad [1]$$

Where: K is the coefficient of shear buckling, which can be given by Eq. [2]:

$$K = \begin{cases} 4\left(\frac{h_w}{a}\right)^2 + 5.34 & \text{For } \frac{a}{h_w} \geq 1 \\ 5.34\left(\frac{h_w}{a}\right)^2 + 4 & \text{For } \frac{a}{h_w} < 1 \end{cases} \quad [2]$$

Hagen et al. [19] conducted numerical simulations to provide design guidelines for predicting the shear resistance of pure shear beams with reinforced and unreinforced web openings. The design shear strength of beams with regularly shaped openings, with and without stiffeners or reinforcement, is given by equation [3]:

$$V_{bw,mod,Rd} = \left(1-\frac{D_h}{h}\right)\chi_w C_2 \frac{f_{yw}}{\gamma_{M1}\sqrt{3}} h\, t \quad < V_{bw,mod\ cutoff,Rd} = \alpha_c\left(1-\frac{D_h}{h}\right)\frac{f_{yw}}{\gamma_{M1}\sqrt{3}} h\, t \quad [3]$$

Where: Dh is the height of the opening and (h) is the clear web height (depth) between flanges and (t) web thickness, C2 is an adjustment factor that account-off factor which equal C2=1 in case of single, non-reinforced circular opening located on the horizontal center line of the girder. And in case of girders with a rectangular or elongated circular opening equal $C_2 = \frac{\sqrt{3}}{\sqrt{4\left(\frac{L}{s_t}\right)^2+3}}$, where L is the cantilevered member length with a shear force V at the fixed end, st height of the web above the opening with thickness (t). αc is cut-off factor is equal $\alpha_c = \left(1-0.32\frac{D_h}{h}\right)$ for all opening, χ_w is the buckling reduction factor for shear as given in EN 1993-1-5 [20] for girders without opening. Azmi

et al. [21] proposed an experimental model to estimate the ultimate shear loading of steel plate containing a circular web opening with vertical and inclined stiffeners by testing the failure of ten simply supported beams under applied shear loads at the centre of gravity of the section. Centrally arranged circular web openings of different diameters are made at five different angles in the middle area of the beam.

On the other hand, Mirambell et al. [22-23] proposed an expression to estimate the critical buckling shear stress and coefficient of tapered plate, taking into account the effect of flange dimensions, and developed an analytical model to evaluate the ultimate shear strength of tapered plate beams. Bedynek et al. [24] classified the tapered plate girder into four types according to the direction of the diagonal tension field formed in the post-buckling stage and the stress state of the inclined flange. Serror et al. [25] presented a study of the effect of different geometric parameters on the elastic shear buckling and nominal shear strength of tapered end webs.

All the above studies were designed to evaluate the shear strength of prismatic plate girders with holes or the shear strength of tapered webs without holes. Various steel design codes, such as AASHTO [26] and AISC [27], rely on experimental and theoretical studies of prismatic members to determine the axial, bending, and shear capacities of web tapered members. EN 1993-1-5 [20] contains design equations for elastic buckling formulations for prismatic webs that can be used for tapered webs, provided that the flange inclination angle (β) does not exceed 10°. When the angle (β) exceeds 10°, the elastic buckling load of the tapered web can be estimated by assuming that it is a rectangular panel based on a web of greater depth. In addition, there are limited studies and no guidance on the shear strength of tapered web girders with perforated webs. In fact, the only study the authors are aware of that addresses this question is Gendy's. [28] presented a numerical analysis to determine the critical shear stress of tapered webs with circular holes. The method is based on the effect of changing the taper value, aspect ratio, and diameter of the circular opening. Furthermore, this study only focuses on a single type of draft and simple boundary conditions for the web, ignoring the effect of flange connections to the web and the t_f/t_w ratio in the proposed equation for shear buckling strength calculations, which this in turn limits its applicability in specific situations. Due to the lack of information on tapered web girders with openings, this paper presents a computational study of the elastic response of such structures and proposes a method for determining the critical shear load of tapered webs with different web opening shapes. The proposed method derives from the elastic buckling strength of tapered stiffened plates in shear and effects of the ratio of opening dimensions respect to the average depth. The proposed method is validated using experimental data. A thoroughly finite element validation was performed using ABAQUS software [29] to provide further assurance that the proposed equations are meaningful and to investigate other factors affecting on the behavior of open-web tapered girders.

2. The Elastic shear buckling equation.

Analytical expressions are given by Timoshenko [18], Eq. [1] obtained the elastic critical shear buckling stress for a rectangular plate, which is a widely used expression. Where the coefficient (k), shear buckling coefficient, depends upon the boundary conditions and the aspect ratio of the web panel, (a/hw), where (a) is the distance between two adjacent transverse stiffeners. Although it has long been recognized that the real boundary conditions at the web-to-flange connection lie between simply supported and fixed, the boundary conditions do it is assumed arbitrarily and conservatively as simple support, mainly due to the lack of means to evaluate it in a reasonable manner. This is one of the main topics of this work when determining the initial shear buckling stress of tapered plate

girders with cut-outs in the web. There are three important factors to consider, which are not included in the formulation of the classical theoretical formula [18]. The first is the effect of tapered angle, and the second is the hole variation (shape and size), a third draft classification of Bedynek et al. [24] of the Real web boundary conditions for the global shear reaction mechanism were recently analysed by Lee and Yoo [30] and Mirambell and Zárate [23] for rectangular and tapered steel plates without openings in the web, respectively. A realistic approach is suggested to determine the elastic shear strength of tapered plates with cut-out. The method is based on the prismatic plate girder technique with openings of Narayanan and Der Avanessian [8] and the tapered plate girder technique without web openings by Bedynek et al. [24]. The elastic shear buckling stress assumption in the web of rectangular plate girder containing openings proposed by Narayanan and Der Avanessian [8-9] can be assumed that the connection along the longitudinal and transverse edge, web panels is clamped above and below the opening due to the higher stiffness of the flange compared to the perforated web. Lee and Yoo [30] proposed a formula for calculating the coefficient (k), which considers the constraint of the web rotation on the flange. as given in equations [7] to Eq. [10]. where (kSF) is the factor when the flange completely restrains the web rotation (no rotational support); (KSS) is the factor when the flange does not restrict the web rotation (free rotational support) as given in equation [2]. [7 and 8]; (tf) is the flange thickness, where the ratio (tf/tw) is the value of both in the equation. [9 and 10] The plate can be considered partially fixed to prevent rotation. Modified critical shear stress τ_{Cr-Mod} can be obtained from equation [4]:

$$\tau_{cr-Mod} = K_{Open}\left(\frac{E\pi^2}{12[1-\upsilon^2]}\right)\left(\frac{t_w}{h_w}\right)^2 \quad [4]$$

Which: $K_{open-Cir} = K\left(1 - \frac{1.5D_o}{\sqrt{(h_w)^2+a^2}}\right)$ For Centrally Located Circular Opening [5]

$$K_{open-S} = K\left(1 - 1.25\sqrt{\frac{A_S}{A_w}}\right)$$ For Centrally Located Square or Rectangular Opening [6]

In which $K_{SF} = 8.98 + 5.61\left(\frac{h_w}{a}\right)^2 - 1.99\left(\frac{h_w}{a}\right)^3$ For $\frac{a}{h_w} \geq 1$ [7]

$$K_{SF} = 5.34\left(\frac{h_w}{a}\right)^2 + 2.31\left(\frac{h_w}{a}\right) + 8.39\left(\frac{a}{h_w}\right) - 3.44 \quad \text{For } \frac{a}{h_w} < 1 \quad [8]$$

$$K = 0.8(K_{SF} - K_{SS})\left(1 - 0.67\left(2 - \frac{t_f}{t_w}\right)\right) \quad \text{For } 0.5 \leq \frac{t_f}{t_w} < 2 \quad [9]$$

$$K = K_{SS} + 0.8(K_{SF} - K_{SS}) \quad \text{For } \frac{t_f}{t_w} \geq 2 \quad [10]$$

which, D_0 = diameter of circular opening; h_w= depth of the web panel; tw = thickness of the web; a = spacing of transverse stiffeners; AS = surface area of the square or rectangular opening; Aw = surface area of the compact web panel ($a \times h_w$).

The above expression has only the effect of presence of web opening circular or rectangular and the real boundary condition between the flange and web, but the effect of tapered web can be developed the above expression of the coefficient of buckling in Eq. [5-10] to:

$$K_{Tapered\&Open} = K_{Open} \times K_{Taper} \quad [11]$$

Which: K_{Taper} is the coefficient of tapering ratio and the type of Typology, k_{open}: is the coefficient of opening, β; is the angle of inclination top or bottom flange, shown in Fig. [1]

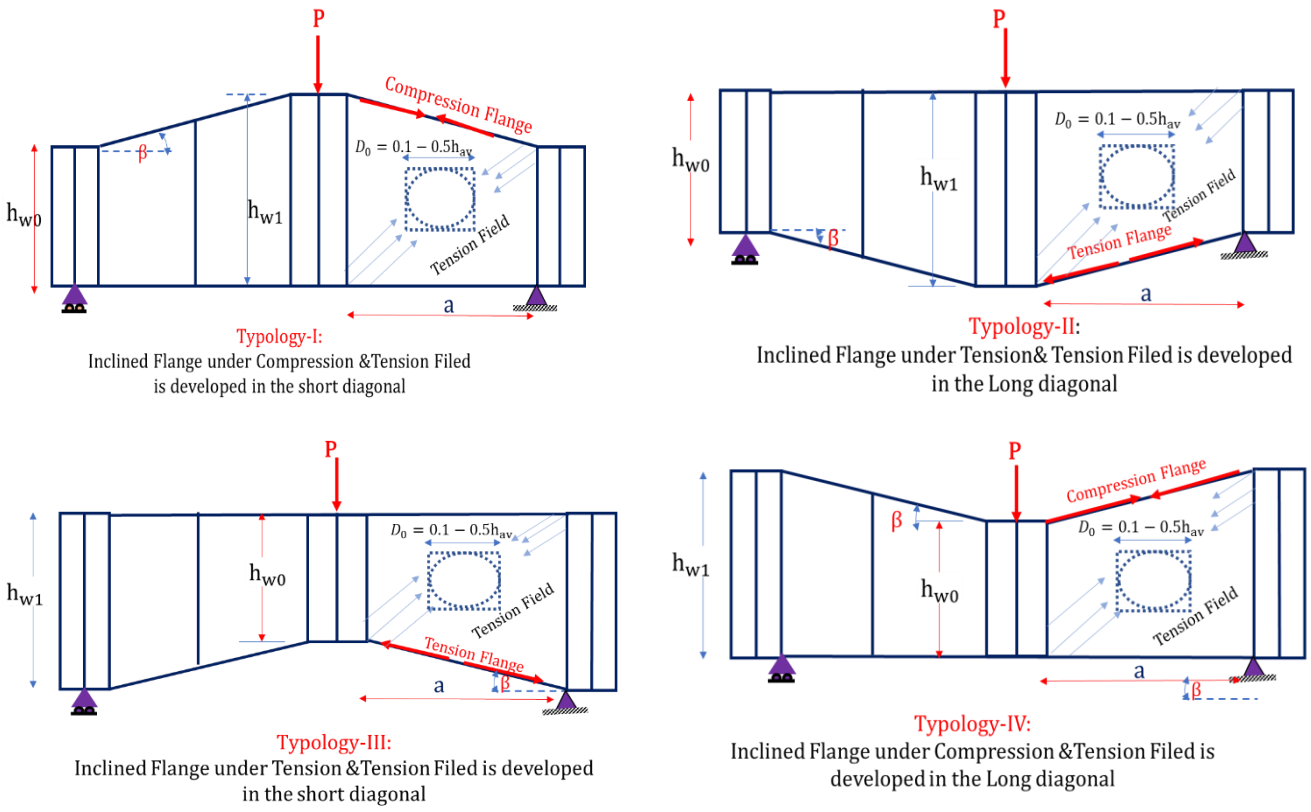

Fig.1. Types of tapered plate girders considered by Bedynek et al. [24] with circular or square opening webs.

3. Finite element modelling and verification.

3-1 Fundamental Modelling Assumptions

In the current study, the commercial software ABAQUS/CAE [29] for finite element modelling was used. The elastic buckling load was calculated for the first positive Eigenmode which responds to the shear buckling mode of a perfectly tapered web girder with circular or square holes as the initial imperfection shape of the I-girder. The S8R5 reduced integration thin shell elements were used in the current bifurcation buckling analysis. The material model of steel for the parametric study is assumed to be elastic-perfectly plastic with elastic modulus, E = 210 GPa, yield stress, Fy = 275 MPa, and Poisson's ratio, υ = 0.3. These numbers are the nominal values for steel grade St 37. However, for models used for validation, material properties conforming to the performed experimental or numerical studies are adopted. The effect of residual stresses is neglected as it was found to have an insignificant effect on the shear strength of plate girders [30]. Experimental data from Azmi et al. [21] and Bedynek et al. [24] were used to obtain numerical models to be examined in numerical parametric studies. To check the validity of the finite element model, the experimental test results are compared with the numerical analysis results, as shown in Sections (3-2-1) and (3-2-2). The current study contains one hundred and seventy six models, as shown in Table (1), covering six main parameters; ratio of diameter of circular and square holes respect to the average height of plate ($\frac{D_0}{h_{w,av}}$ and $\frac{b_s}{h_{w,av}}$), typologies of the tapered web plate, flange to web thickness ratio $\frac{t_f}{t_w}$,, inclination angle of the upper or lower edges (tan β), height to thickness ratio $\left(\frac{h_w}{t_w}\right)$ and normalized plate length $\alpha = \frac{a}{h_w}$ .Fig. 2(a-b) shows the geometric configuration of the plate girders considered herein with single opening in the centre. the focus of the current study is tapered web containing

opening in the centre of the web. The larger depth (hw1) of the web is assumed constant two value for two groups of aspect ratio (A and B) and equals to 800 and 1200mm respectively whereas the smaller depth of the web hw0 varies from 680 to 400 mm for group (A) and varies from 850 to 300 for group (B). The flange width (bf) is having two values as the group model (A or B) and assumed 180 and 250 mm respectively. These numbers are selected to resemble the experimental test by Bedynek et al. [24]. Herein, tapered web types I and II are considered, in which type I, the compression chord is inclined, and the principal compressive stress is applied to the web along the shorter diagonal direction (see Fig. 2-a-b) and type II, the tension chord is inclined and the principal compressive stress in the web starts in the longer diagonal direction (see Fig. 2-c-d). The top chord is laterally braced, to exclude lateral torsional buckling failure modes. On the other hand, the spans and dimensions of the plate bracing, and stiffeners are chosen such that failure is essentially governed by the shear capacity of the end webs, and failure modes due to bending moments, web paralysis buckling, and stiffener yielding are eliminated.

Table 1: Details of the FE Analysis

Parameter	Circular Hole		Square Hole	
	Typology I	Typology II	Typology I	Typology II
Ratio of Diameter of circular or square hole to average depth $\frac{D_0}{h_{av}}$ $\frac{b_s}{h_{av}}$	$0.1h_{av}$ to $0.5h_{av}$ Zero means no hole		$0.1h_{av}$ to $0.5h_{av}$ Zero means no hole	
Normalized plate length $\alpha = \frac{a}{hw_1}$	1.0 and 2.0 Group (A-B)		1.0 and 2 Group (A-B)	
Tapering angle $\tan \beta$	0- 0.15-0.25-0.4 and 0.5 where tan β=0 means no tapering angle (prismatic web)			
$\frac{t_f}{t_w}$	2 and 3.75			
$\frac{h_w}{t_w}$	Ranged from $\frac{2500}{\sqrt{f_y}}$ to $\frac{4000}{\sqrt{f_y}}$			

To reduce numerical error, an h-refinement procedure is conducted in which the size of elements is progressively halved from 150 × 150 mm to 30 × 30 mm. The elastic buckling stress, τcr is then compared to theoretical values as per Timoshenko and Gere [18] for simply supported and Lee [30] with 80% fixation. Based on the performed mesh sensitivity analysis, the element size is taken 30 × 30 mm through the presented study, as shown in Fig. (3). The circular hole and the square hole at the centre of the plate to avoid any fabrication errors. as mentioned by Carlo et al [11] the location of the opening has a great effect on the critical shear load especially when the opening is in the compression zone. A convergence study performed for the pure shear loading considered in this paper for a simply supported web panel where the longitudinal edges are restrained by flanges. The number of elements in the transverse direction ranges from 50 to 10 then the resulted elastic buckling load has been compared with the closed-form solution established by Timoshenko and Gere [18] and Lee and Yoo [30]. However, the elements have an aspect ratio of approximately 1.002 to avoid the problem of convergence. When the size of elements was 30 the percentage of error was 1.002% for shear.

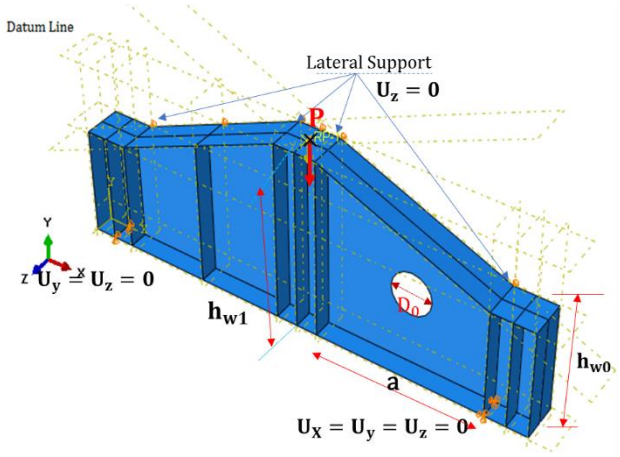

(a)- Typology I- Circular Opening

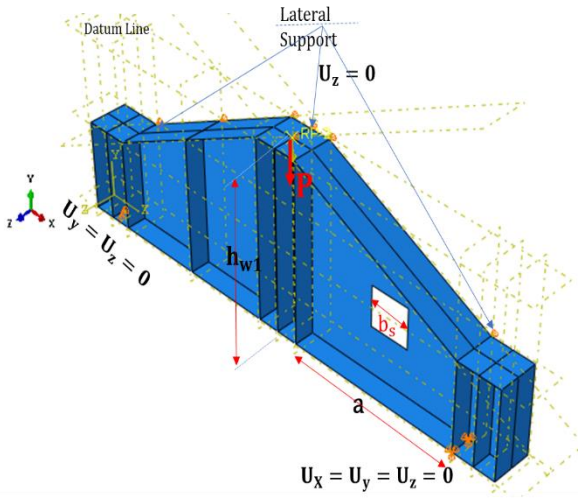

(b)- Typology I- Square Opening

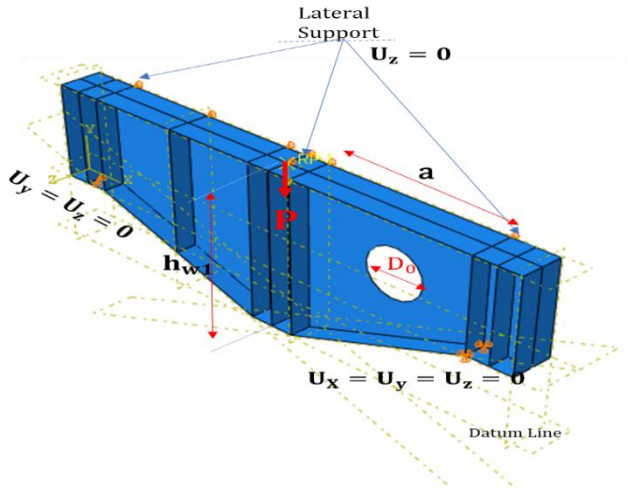

(c)- Typology II- Circular Opening

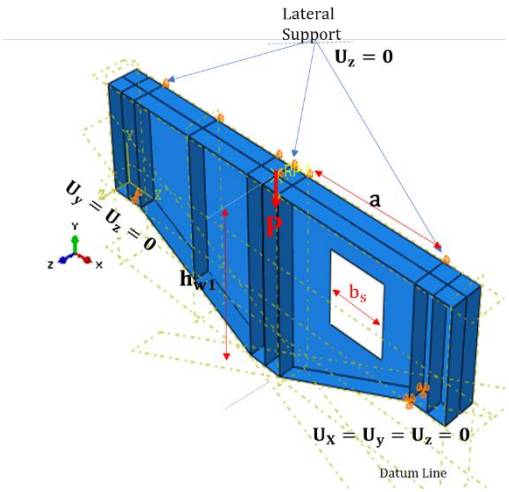

(d)- Typology II- Square Opening

Fig. (2): Finite Element model: Supports restraints and lateral bracing

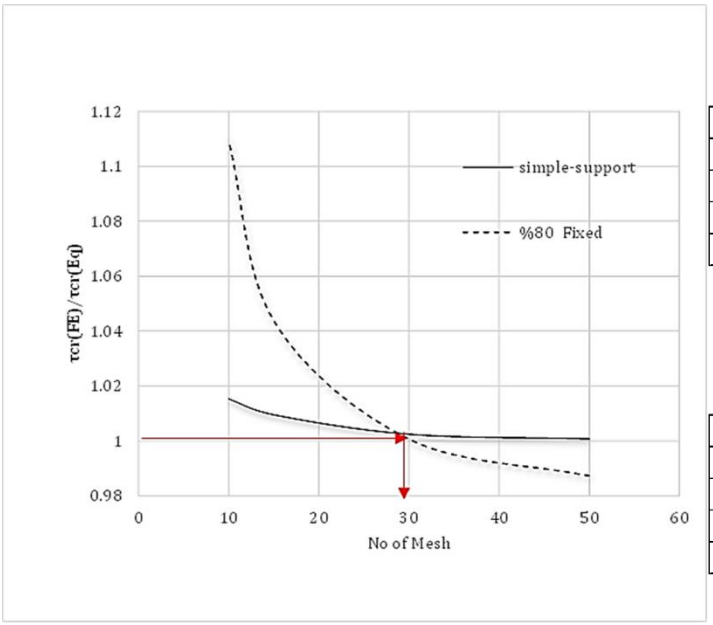

Verification 1: Comparison between Simple support (τ_{cr} *by Timoshinko* [18]*and Abaqus* [29]

Mesh No	Mesh Size (mm)	τcr (FE)	τcr (Eq)	τcr (FE)/τcr Eq
50	30	28.403	28.33497	1.0024
30	50	28.605	28.33497	1.00953
15	100	28.77	28.33497	1.01535
10	150	30.34	28.33497	1.07076

Verification 2: Comparison between- %80 Fixation τ_{cr} *by Lee and Yoo*[28]*and Abaqus* [29]

Mesh No	Mesh Size	τcr (FE)	τcr (Eq)	τcr (FE)/τcr Eq
50	30	194.83	197.344	0.98726
30	50	197.47	197.344	1.00064
15	100	205.98	197.344	1.04376
10	150	218.95	197.344	1.10948

Fig (3): Convergence study of mesh size

3-2 Validation of models

To the best of the author's knowledge, no experimental test data exists for tapered girders with opening in the webs. However, experimental data does exist for tapered girders without openings webs and is used to provide a measure of confidence in the proposed equations. Finite element results are validated by comparison to available experimental and numerical work. Validation is performed considering the experimental work performed by Azmi et al. [21] on flat plate girders with a circular hole, in addition to the experimental and numerical work on tapered plate girders performed by Bedynek et al. [24].

3-2-1 Validation using experimental data in Azmi et al. [21]

The web plates tested by Azmi et al. [21] were composed of steel grade S275 having a yield strength of 295.1 MPa and 304.9 for the web and the flange plates respectively. Young's modulus (E) is equal to 205.5GPa and 209.8 for the web and the flanges plates respectively and Poisson's ratio (υ) is equal to 0.3. The critical load (Vcr) and the ultimate shear strength (Vu) computed from the finite element model for each plate girder is compared to the test and analytical results reported by Azmi et al. [21] as shown in Table 2. The results of the finite element model are compatible with both experimental and analytical results with an average difference of 6.8%. Von-Misses stresses at limit load are compared with the failure shapes of the tested specimens in Fig. (4).

Table 2: Comparison between FE (ABAQUA) and Experimental and Analytical Results Reported by Azmi et al. [21] (Results are in kN).

Girder	Results by Azmi et al. [15]			Results by FE Abaqus		% Difference
	$V_{u\,(Exp)}$ kN	$V_{u\,(FE)}$ kN	$\frac{V_{u(FE)}}{V_{u(EXP)}}$	$V_{u\,(Abaqus)}$ KN	$\frac{V_{u(Abaqus)}}{V_{u(EXP)}}$	
PG-90-Cr100	187.7	192.6	1.026	200.0	1.06	6.5
PG-90-Cr200	126.4	138.2	1.093	135.5	1.07	7.1
Average difference						6.8

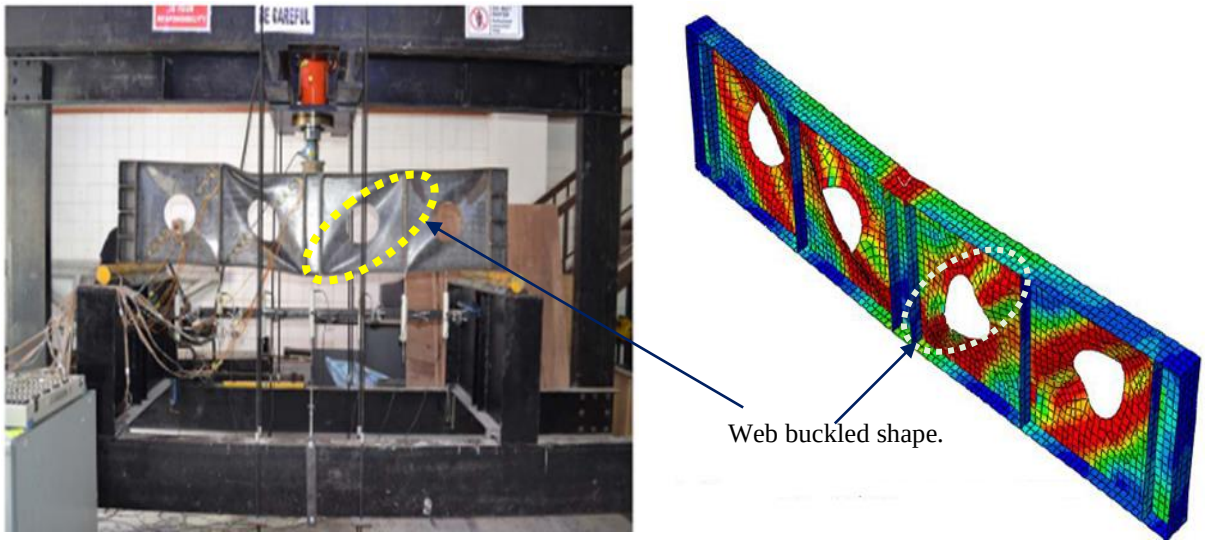

a- PG-90-Cr200

Fig. (4). Plot of Von-Mises in Abaqus vs. Experimental Test Failure by Azmi et al. [21]

3-2-2 Validation using experimental data in Bedynek [24]

Validation is also performed against results reported by Bedyneket al. [24] for a set of tapered plate girders. All plate girders were composed of steel S275 with a yield strength of 320.6 MPa, the ultimate strength of 423.4 MPa, Young's modulus (E) of 211.3 GPa, and Poisson's ratio (υ) of 0.3. All tested girders of Bedynek et al. [24] are of Model Type (A). The critical load (V_{cr}) computed numerically by Bedynek et al. [24], VcrFE is compared to that obtained by test (V_{crEXP}) and the critical shear load computed herein from the first eigen-value using ABAQUS ($V_{crAbaqus}$), also to obtain the deformed shape for the critical shear load as the first eigen-value. In addition, the ultimate shear strength obtained from the finite element model for each plate girder ($V_{u\ Abaqus}$) Results are listed in Table 3 showing perfect agreement between test results and numerical solutions. Results of the finite element model are compatible with both the experimental tests and analytical results with an average difference of 3.53% from test results. Fig. (5) compares the buckled shape of the web as extracted from the model against the experimental test. Good agreement can be observed. The presented validation effort provides confidence in the modeling approach described earlier in simulating the buckling and post-buckling behavior of prismatic girders with circular holes and tapered end web panels in steel plate girders.

Table 3: Comparison between FE (ABAQUS) and Experimental and Analytical Results Reported by Bedynek et al. [24] (Results are in kN).

Girder	Results by Bedynek. [24]				Results by FE (Abaqus)				% Difference
	V_{cr} (Exp) kN	V_u (Exp) kN	V_{cr} (FE) kN	Vu (FE) kN	Vcr (Abaqus) kN	Vu (Abaqus) kN	$\frac{V_{cr(FE)}}{V_{cr(EXP)}}$	$\frac{V_{u(Abaqus)}}{V_{u(EXP)}}$	
A_600_800_800_4_180_15	225.0	392.0	223.9	410.8	223.13	384.24	0.99	0.98	1.94
B_500_800_1200_4_180_15	220.0	320.5	212.0	346.5	213.0	330.34	0.97	1.03	3.07
C_480_800_800_4_180_15	265.0	388.2	269.1	408.7	261.4	410.5	0.98	1.05	5.74
Average Difference%									3.53

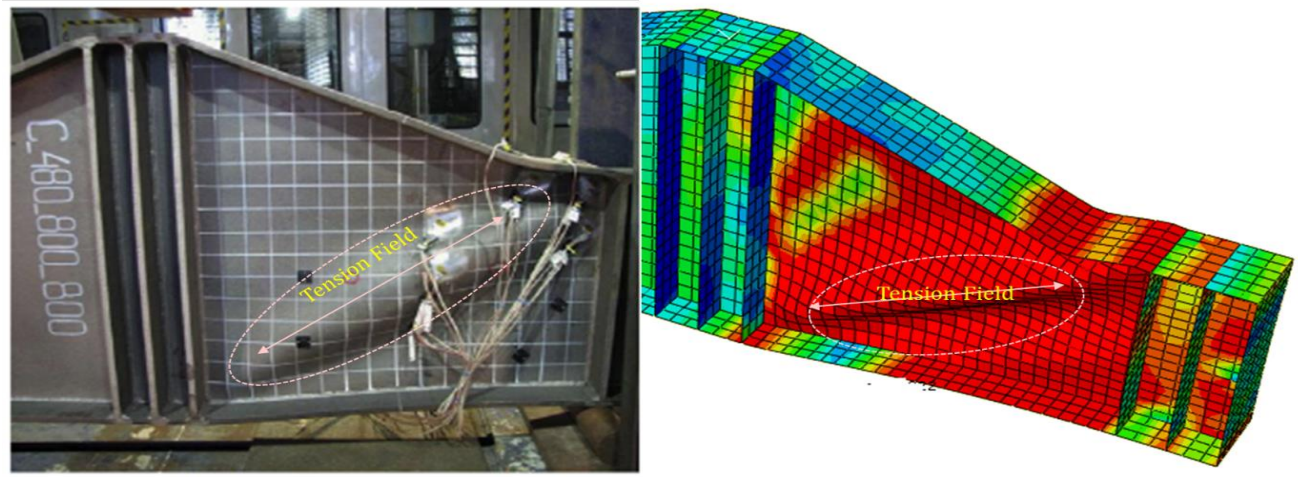

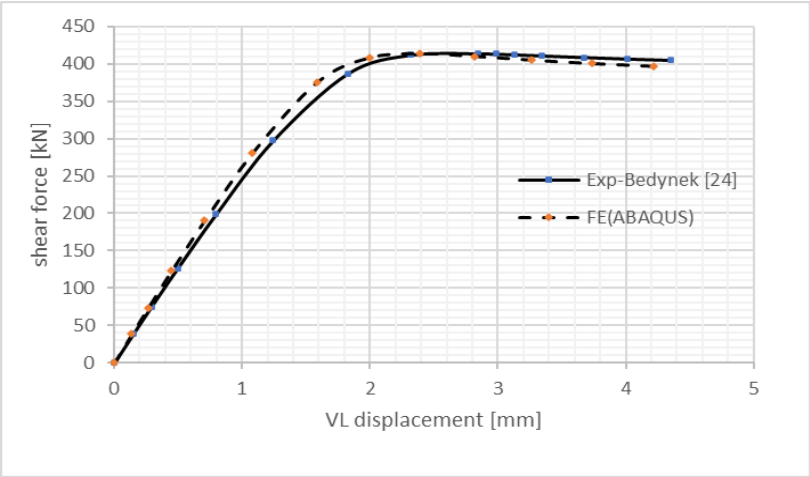

Shear load vs vertical displacement

Fig.(5): Deformed Shape Of Girder (C) tested by Bedynek et al. [24] Vs FE Abaqus

4. Parametric study

Full-scale tapered plate girders containing holes loaded under mid-span concentrated loads of typologies I and II as shown in (Fig. 1 and 2) were generated in this paper. The safety of the constructed bridges was confirmed by three-dimensional finite element analysis and loading experiments [21] and [24]. Therefore, this parametric study was generated to substitute the lack of available design shear strengths of the tapered web having holes Table (4) provides the details and FE results of the tapered plate girder with circular and square opening with Typology I and II.

Currently, 3D FE models, using ABAQUS [29] FE package, were performed on one hundred and seventy-six tapered girders with circular or square holes which cover the following parameters:

1- The ratio of the dimensions of the hole to the average height of the web ($\frac{D_o}{h_{w,av}}$ and $\frac{b_s}{h_{w,av}}$)

2- Angle of the inclined flanges (tan β); (0, 0.15, 0.25, 0.40 and 0.50)

3- Aspect ratio of the web panels ($\alpha = \frac{a}{h_w}$); (1.0 and 2.0) and

4- web thickness (4 and 6mm)

5- Slenderness ratio is ranged between ranged from $\frac{2500}{\sqrt{f_y}}$ to $\frac{4000}{\sqrt{f_y}}$

Table 4: Geometric properties of Group A and B

Type	Girder	Geometrical properties									
		h_0 mm	h_1 mm	t_w mm	a mm	t_f mm	b_w mm	$\alpha = \frac{a}{h_w}$	tan β	β°	h_{av} mm
Prismatic	P-A-Cr-0-0hav	800	800	4 and 6	800	15	180	1	0	0	800
	P-B-Cr-0-0hav	1200	1200	4 and 6	2400	25	250	2	0	0	1200
Typology I-II Group (A)	I-II-A-Cr-0.15-0hav	680	800	4 and 6	800	15	180	1	0.15	8.5	740
	I-II-A-Cr-0.25-0hav	600	800	4 and 6	800	15	180	1	0.25	14	700
	I-II-A-Cr-0.4-0hav	480	800	4 and 6	800	15	180	1	0.4	21.8	640
	I-II-A-Cr-0.5-0hav	400	800	4 and 6	800	15	180	1	0.5	26.6	600

Typology I-II Group (B)	I-II-B-Cr-0.15-0hav	840	1200	4 and 6	2400	25	250	2	0.15	8.5	1025
	I-II-B-Cr-0.25-0hav	600	1200	4 and 6	2400	25	250	2	0.25	14	900
	I-II-B-Cr-0.4-0hav	300	1200	4 and 6	2400	25	250	2	0.375	20.5	750

Note: I-A-Cr-0.15-0.1hav: I refer to number of typology (Prismatic, Typology-I or Typology- II), A refers to group of models as aspect ratio (group (A) α=1 and group (B) α=2), Cr refers to circular hole, Sr refers to square hole, 0.15 refers to tan β the inclination of upper or lower flange, 0.0hav refers Dimension of hole average height of web

Table 5 Critical shear buckling loads for Prismatic and Typology with circular and square hole for group (A) and (B).

Type	Girder	Geometrical properties				Results		
		$\alpha = \frac{a}{h_w}$ [1]	tan β [2]	h_{av} mm [3]	D_0 Or b_{sq} mm [4]	Vcr (FE) kN [5]	Vcr Pro.Eq(18) kN [6]	[5]/[6]
Prismatic	P-A-Cr-0-0hav	1	0	800	0	191.75	182.69	1.05
Circular Hole	P-A-Cr-0-0.1hav				80	173.4	161.59	1.07
Group (A)	P-A-Cr-0-0.2hav				160	145.25	140.91	1.03
	P-A-Cr-0-0.3hav				240	122.6	120.63	1.02
	P-A-Cr-0-0.4hav				320	103.3	100.75	1.03
	P-A-Cr-0-0.5hav				400	88.75	81.29	1.09
Prismatic	P-A-Sr-0-0.1hav	1	0	800	80	166.5	158.17	1.05
Square Hole	P-A-S-0-0.2hav				160	134.3	134.13	1.01
Group (A)	P-A- Sr -0-0.3hav				240	109.5	110.57	0.99
	P-A- Sr -0-0.4hav				320	91.4	87.50	1.04
	P-A- Sr -0-0.5hav				400	166.5	64.90	1.23
Prismatic	P-B-Cr-0-0hav	2	0	1200	0	97.1	90.74	1.07
Circular Hole	P-B-Cr-0-0.1hav				120	96.1	85.77	1.12
Group (B)	P-B-Cr-0-0.2hav				240	90.05	80.88	1.11
	P-B-Cr-0-0.3hav				360	82.6	76.08	1.08
	P-B-Cr-0-0.4hav				480	76	71.37	1.06
	P-B-Cr-0-0.5hav				600	68	66.74	1.02
Prismatic	P-B-Sr-0-0.1hav	2	0	1200	120	91	91.88	0.99
Square Hole	P-B-Sr-0-0.2hav				240	77.2	82.11	0.94
Group (B)	P-B- Sr -0-0.3hav				360	64.1	72.52	0.88
	P-B- Sr -0-0.4hav				480	53.3	63.12	0.84
	P-B- Sr -0-0.5hav				600	45.06	53.90	0.84
Typology I	I-A-Cr-0.15-0hav	1	0.15	740	0	215.1	228.85	0.94
Circular Hole	I-A-Cr-0.15-0.1hav				74	197.15	200.24	0.98
	I-A-Cr-0.15-0.2hav				148	166.13	172.97	0.96
	I-A-Cr-0.15-0.3hav				222	138.53	147.04	0.94
	I-A-Cr-0.15-0.4hav				296	114.75	122.45	0.94
	I-A-Cr-0.15-0.5hav				370	96.2	99.19	0.97
	I-A-Cr-0.25-0hav	1	0.25	700	0	238.45	259.62	0.92
	I-A-Cr-0.25-0.1hav				70	219.79	226.36	0.97
	I-A-Cr-0.25-0.2hav				140	186.14	194.98	0.95
	I-A-Cr-0.25-0.3hav				210	157.72	165.48	0.95

Type	Girder	Geometrical properties				Results		
		$\alpha = \frac{a}{h_w}$ [1]	tan β [2]	h_{av} mm [3]	D_0 Or b_{sq} mm [4]	Vcr (FE) kN [5]	Vcr Pro.Eq(18) kN [6]	$\frac{[5]}{[6]}$
	I-A-Cr-0.25-0.4hav				280	133.9	137.85	0.97
	I-A-Cr-0.25-0.5hav				350	115.9	112.10	1.03
	I-A-Cr-0.4-0hav	1	0.4	640	0	289.65	305.769	0.94
	I-A-Cr-0.4-0.1hav				64	265.7	266.10	0.99
	I-A-Cr-0.4-0.2hav				128	227.5	228.97	0.99
	I-A-Cr-0.4-0.3hav				192	187.4	194.39	0.96
	I-A-Cr-0.4-0.4hav				256	154.5	162.35	0.95
	I-A-Cr-0.4-0.5hav				320	128.5	132.86	0.96
	I-A-Cr-0.5-0hav	1	0.5	600	0	336	336.54	0.99
	I-A-Cr-0.5-0.1hav				60	312.85	292.95	1.07
	I-A-Cr-0.5-0.2hav				120	267.8	252.27	1.06
	I-A-Cr-0.5-0.3hav				180	212.45	214.50	0.99
	I-A-Cr-0.5-0.4hav				240	180.45	179.63	1.01
	I-A-Cr-0.5-0.5hav				300	147.5	147.67	0.99
Typology I	I-A- Sr -0.15-0.1hav	1	0.15	740	074	191.7	196.35	0.97
Square Hole	I-A- Sr -0.15-0.2hav				148	158.95	165.43	0.96
	I-A- Sr -0.15-0.3hav				222	127.27	136.08	0.94
	I-A- Sr -0.15-0.4hav				296	103.5	108.33	0.96
	I-A- Sr -0.15-0.5hav				370	88.1	82.14	1.07
	I-A- Sr -0.25-0.1hav	1	0.25	700	70	212.95	222.23	0.96
	I-A- Sr -0.25-0.2hav				140	174.5	187.05	0.93
	I-A- Sr -0.25-0.3hav				210	138.75	154.08	0.90
	I-A- Sr -0.25-0.4hav				280	111.7	123.31	0.91
	I-A- Sr -0.25-0.5hav				300	92.3	94.76	0.97
	I-A- Sr -0.4-0.1hav	1	0.4	640	64	260.25	261.69	0.99
	I-A- Sr -0.4-0.2hav				128	208.5	220.61	0.94
	I-A- Sr -0.4-0.3hav				192	165.1	182.53	0.90
	I-A- Sr -0.4-0.4hav				256	133.2	147.46	0.90
	I-A- Sr -0.4-0.5hav				320	106.65	115.38	0.92
	I-A- Sr -0.5-0.1hav	1	0.5	600	60	305.4	288.43	1.06
	I-A- Sr -0.5-0.2hav				120	245.9	243.75	1.01
	I-A- Sr -0.5-0.3hav				180	194	202.49	0.96
	I-A- Sr -0.5-0.4hav				240	155.5	164.66	0.94
	I-A- Sr -0.5-0.5hav				300	126.5	130.25	0.97
Ave								**1.02**

Table 6: Critical shear buckling loads for Typology II with circular and square hole for group (A) and (B).

Type	Girder	Geometrical properties				Results		
		$\alpha = \frac{a}{h_w}$ [1]	tan β [2]	h_{av} mm [3]	D_0 Or b_{sq} mm [4]	Vcr (FE) kN [5]	Vcr Pro. Eq (18) kN [6]	[5]/[6]
Typology II	II-A-Cr-0.15-0hav	1	0.15	740	0	201.35	211.19	0.95
Circular Hole	II-A-Cr-0.15-0.1hav				74	185.5	186.50772	0.99
	II-A-Cr-0.15-0.2hav				148	156.5	162.68	0.96
	II-A-Cr-0.15-0.3hav				222	132.5	139.73	0.95
	II-A-Cr-0.15-0.4hav				296	112.3	117.62	0.95
	II-A-Cr-0.15-0.5hav				370	96	96.39	0.99
	II-A-Cr-0.25-0hav	1	0.25	700	0	216.7	236.04	0.92
	II-A-Cr-0.25-0.1hav				70	200	207.72	0.96
	II-A-Cr-0.25-0.2hav				140	169.85	180.71	0.94
	II-A-Cr-0.25-0.3hav				210	144.5	155.01	0.93
	II-A-Cr-0.25-0.4hav				280	122	130.62	0.93
	II-A-Cr-0.25-0.5hav				350	104.3	107.56	0.97
	II-A-Cr-0.4-0hav	1	0.4	640	0	258	273.31	0.94
	II-A-Cr-0.4-0.1hav				64	240.5	239.97	1.00
	II-A-Cr-0.4-0.2hav				128	206.6	208.52	0.99
	II-A-Cr-0.4-0.3hav				192	174.5	178.94	0.97
	II-A-Cr-0.4-0.4hav				256	146.5	151.25	0.96
	II-A-Cr-0.4-0.5hav				320	122.75	125.44	0.97
	II-A-Cr-0.5-0hav	1	0.5	600	0	305.85	298.15	1.02
	II-A-Cr-0.5-0.1hav				60	287.5	261.76	1.09
	II-A-Cr-0.5-0.2hav				120	247.4	227.57	1.08
	II-A-Cr-0.5-0.3hav				180	208.2	195.56	1.06
	II-A-Cr-0.5-0.4hav				240	173.33	165.75	1.05
	II-A-Cr-0.5-0.5hav				300	143.45	138.12	1.03
Typology II	II-A- Sr -0.15-0.1hav	1	0.15	740	074	179.9	182.88	0.98
Square Hole	II-A- Sr -0.15-0.2hav				148	145.5	155.59	0.93
	II-A- Sr -0.15-0.3hav				222	118.45	129.32	0.91
	II-A- Sr -0.15-0.4hav				296	98.4	104.06	0.94
	II-A- Sr -0.15-0.5hav				370	85.25	79.82	1.067
	II-A- Sr -0.25-0.1hav	1	0.25	700	70	195	203.92	0.95
	II-A- Sr -0.25-0.2hav				140	157	173.35	0.90
	II-A- Sr -0.25-0.3hav				210	128	144.33	0.88
	II-A- Sr -0.25-0.4hav				280	106.25	116.86	0.91
	II-A- Sr -0.25-0.5hav				300	88.5	90.93	0.97

Type	Girder	Geometrical properties				Results		
		$\alpha = \frac{a}{h_w}$ [1]	tan β [2]	h_{av} mm [3]	D_0 Or b_{sq} mm [4]	Vcr (FE) kN [5]	Vcr Pro. Eq (18) kN [6]	[5]/[6]
	II-A- Sr -0.4-0.1hav	1	0.4	640	64	234	236.0	0.99
	II-A- Sr -0.4-0.2hav				128	191.4	200.91	0.95
	II-A- Sr -0.4-0.3hav				192	154.75	168.04	0.92
	II-A- Sr -0.4-0.4hav				256	127.5	137.38	0.92
	II-A- Sr -0.4-0.5hav				320	104	108.94	0.95
	II-A- Sr -0.5-0.1hav	1	0.5	600	60	279	257.73	1.08
	II-A- Sr -0.5-0.2hav				120	229.5	219.9	1.043
	II-A- Sr -0.5-0.3hav				180	183.3	184.62	0.99
	II-A- Sr -0.5-0.4hav				240	151.5	151.94	0.99
	II-A- Sr -0.5-0.5hav				300	124.5	121.8	1.02
Ave								0.97

5. RESULT AND DESCUSSION

The buckling coefficient (*k*) has been proposed as Eq. [10] as shown in section (2). Table (5 and 6) listed the results of critical shear load resulted from finite element analysis ($V_{cr.FE}$) listed in column [5] in Table [5] and Table [6], which indicated in section (5-3) Equation (18).

5-1 Effects of ($\frac{D_0}{h_{av}}$ or $\frac{b_s}{h_{av}}$) for Circular and square Holes

The deformed shape of the first eigen-buckling mode shown in Fig. [6] and Fig. [7] illustrated that the buckling of steel plate girders with web openings undergoes three different modes of load carrying mechanism. The first mode, when the web buckles, the shear stress reaches its critical value(τ_{Cr-Mod}), which observed in the opening web girders tested by Narayanan and Rockey [8]. Also, the buckled shape of the tension field action is appeared in the short direction in the two cases of opening (circular and square) in case of Typology-I, shown in Fig. [6-a and b]. Additionally, it was appeared in the long direction in the two cases of opening (circular and square) in case of Typology-II, shown in Fig. [7-a and b]. on the other hand, Fig. [8] and Fig. [9] show the relation between the variation of normalized critical load ($\frac{V_{cr}}{V_y}$) obtained from elastic analysis described before as $\frac{D_0}{h_{av}}$ and $\frac{b_s}{h_{av}}$ changed for Typology (I) and Typology (II) with aspect ratio α=1 and 2, for two shape of holes circular and square. As shown, there is a clear negative correlation between $\frac{D_0}{h_{av}}$ or $\frac{b_s}{h_{av}}$and ($\frac{V_{cr}}{V_y}$) for various value of tapering angle from prismatic (tan β = 0) to tapered with (tan β = 0.5). In terms of that, increasing $\frac{D_0}{h_{av}}$ or $\frac{b_s}{h_{av}}$ from 0.1 to 0.5 for circular and square hole in two type of tapering (Typology I and Typology II) yields to a significant reduction in ($\frac{V_{cr}}{V_y}$) by 57% and 52% respectively. But the increasing of tapering angle from (tan β=0) to (tan β=0.5) with increasing the $\frac{D_0}{h_{av}}$ or $\frac{b_s}{h_{av}}$ effect on the ($\frac{V_{cr}}{V_y}$) by increasing the value by 59%.

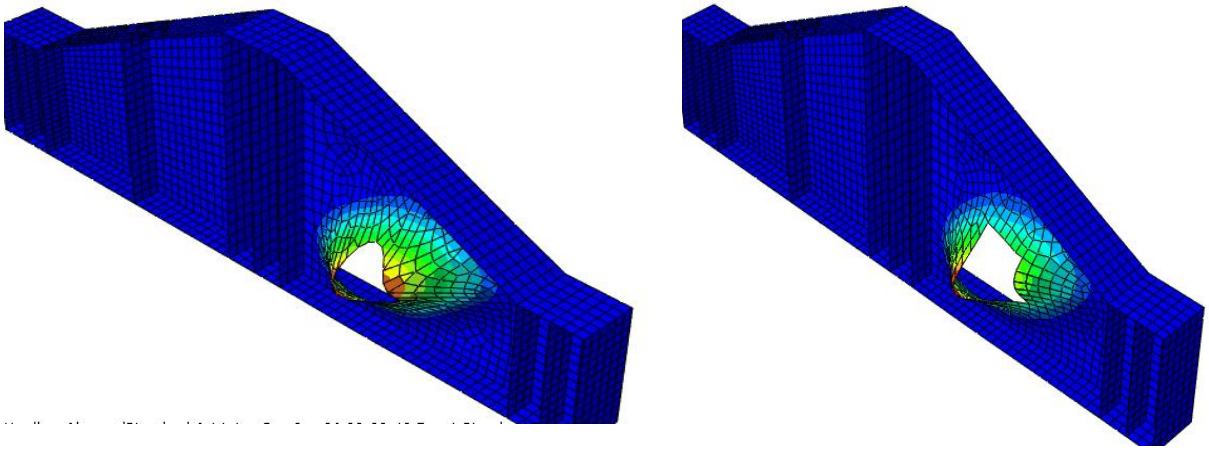

a- Circular opening b- Square opening

Fig. [6]: Deformed shape of the first Eigan-mode for Typology-I girder in case of $\frac{D_o}{h_{av}}$ or $\frac{b_s}{h_{av}}$ =0.3

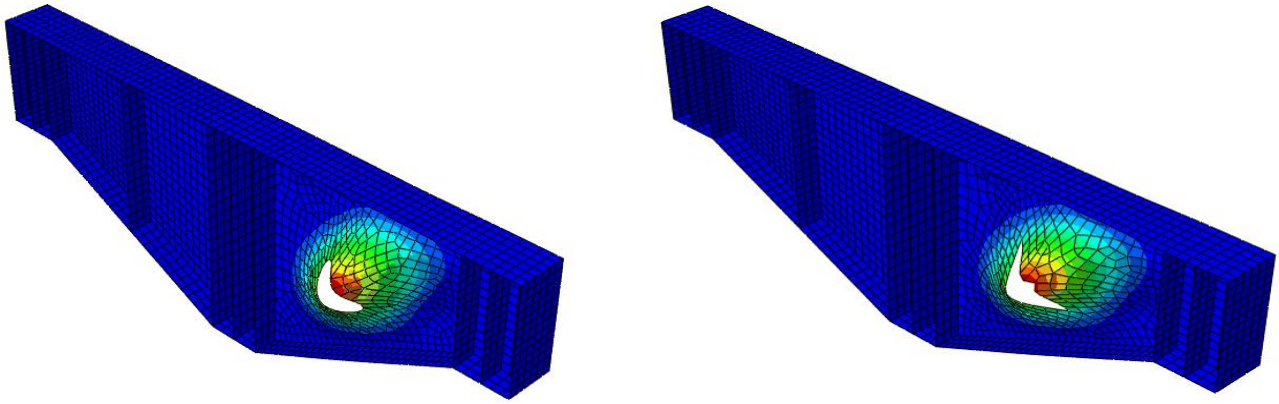

a- Circular opening b- Square opening

Fig. [7]: Deformed shape of the first Eigan-mode for Typology-II girder in case of $\frac{D_o}{h_{av}}$ or $\frac{b_s}{h_{av}}$ =0.3

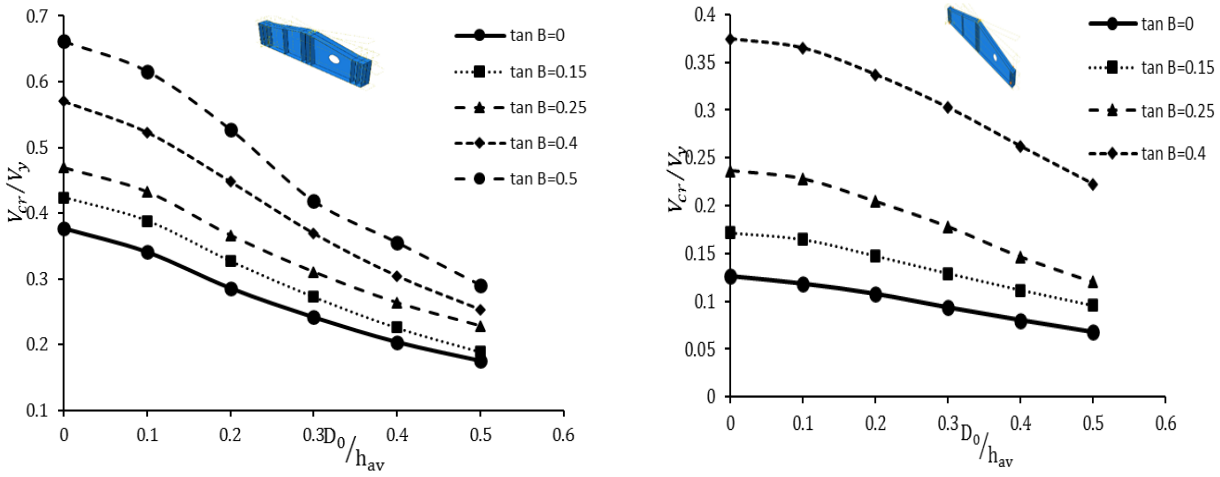

α=1 **α=2**

(a)- Circular Hole

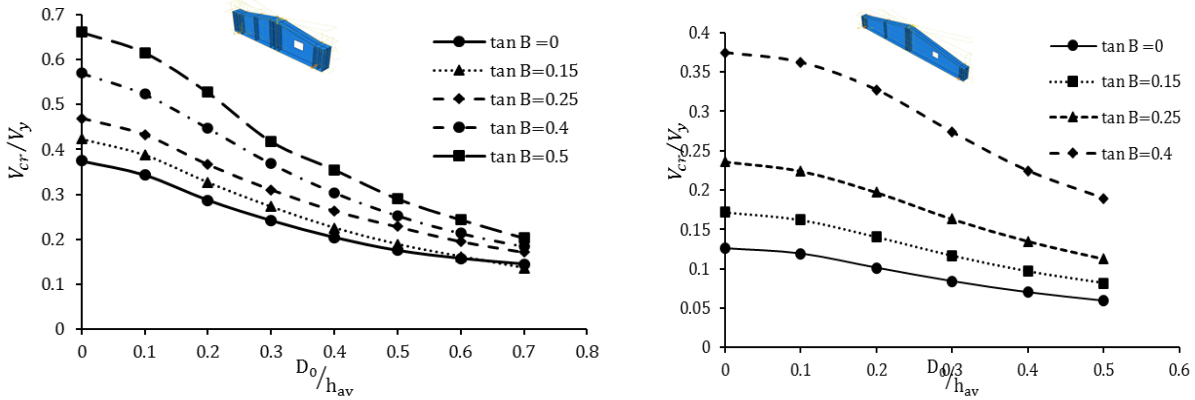

α=1 **α=2**

(b) Square Hole

Fig. (8): Effect of ($\frac{D_0}{h_{av}}$) with different value of tapered angle (tan β) on ($\frac{V_{cr}}{V_y}$) Typology-I

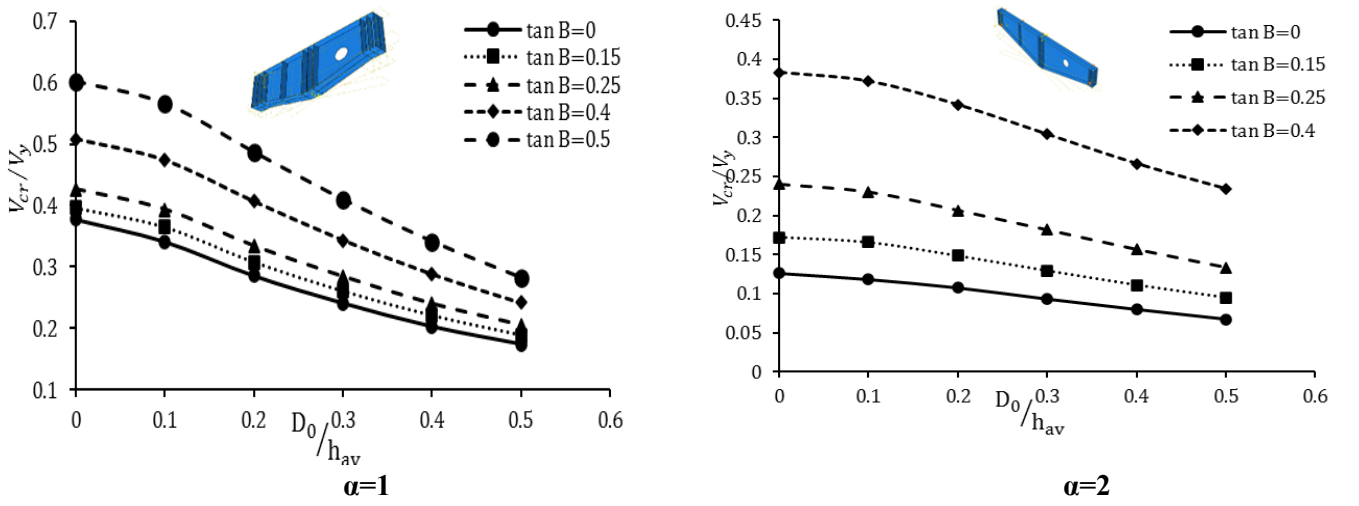

α=1 **α=2**

(a) Circular Hole

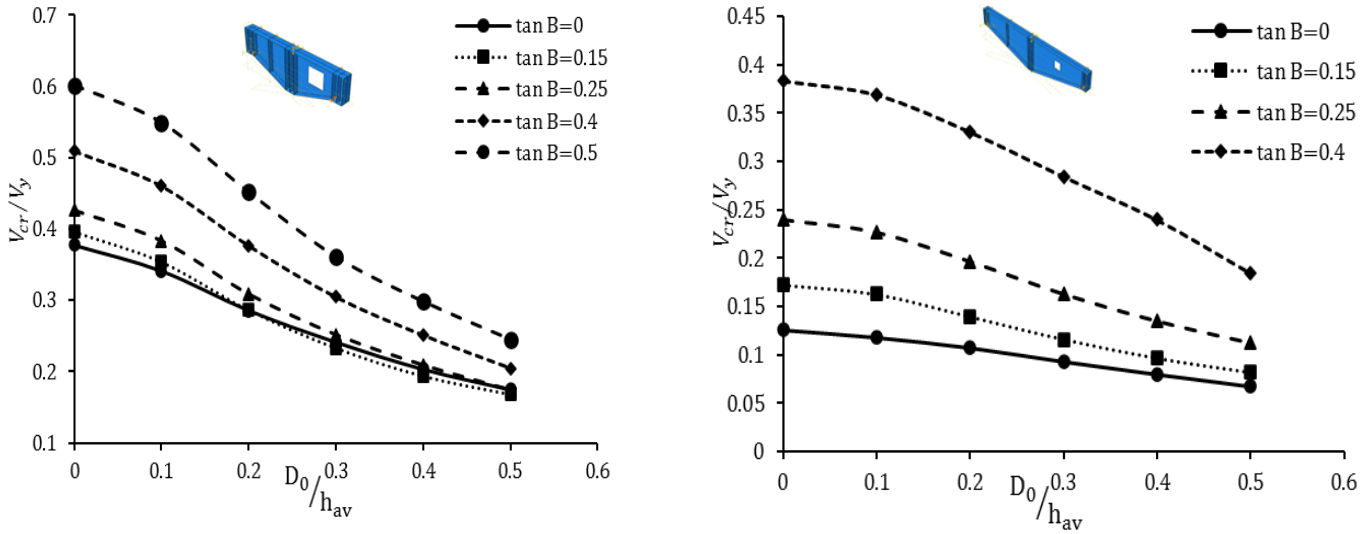

α=1 **α=2**

(b) Square Hole

Fig. (9): Effect of ($\frac{D_0}{h_{av}}$) with different value of tapered angle (tan β) on ($\frac{V_{cr}}{V_y}$) Typology-II

5-2 Effect of tapering angle (tan β)

Fig. (10) and Fig. (11) illustrate the increase of ($\frac{V_{cr}}{V_y}$) when plotted against tan β for different value of $\frac{D_0}{h_{av}}$ in circular hole and $\frac{b_s}{h_{av}}$ for square hole. When the tapering angle (θ) increases from tan β=0.0 to tan β=0.50, the normalized critical load ($\frac{V_{cr}}{V_y}$) increases by 72% on average. Meanwhile; for $\frac{D_0}{h_{av}}$= 0 in circular hole, when tan β increases from tan β=0.0 to tan β=0.5, the normalized critical load ($\frac{V_{cr}}{V_y}$) increases by 75% on average and for $\frac{b_s}{h_{av}}$= 0.3 in square hole, when tan β increases from tan β=0.0 to tan β=0.5, the normalized critical load ($\frac{V_{cr}}{V_y}$) increases by 73% on average. It is found that the increase of tapering angle led to increasing the elastic buckling load due to reduction of compression diagonal length. Moreover, the normalized critical load ($\frac{V_{cr}}{V_y}$) becomes more sensitive to tapering angle β when $\frac{D_0}{h_{av}}$ or $\frac{b_s}{h_{av}}$ increases.

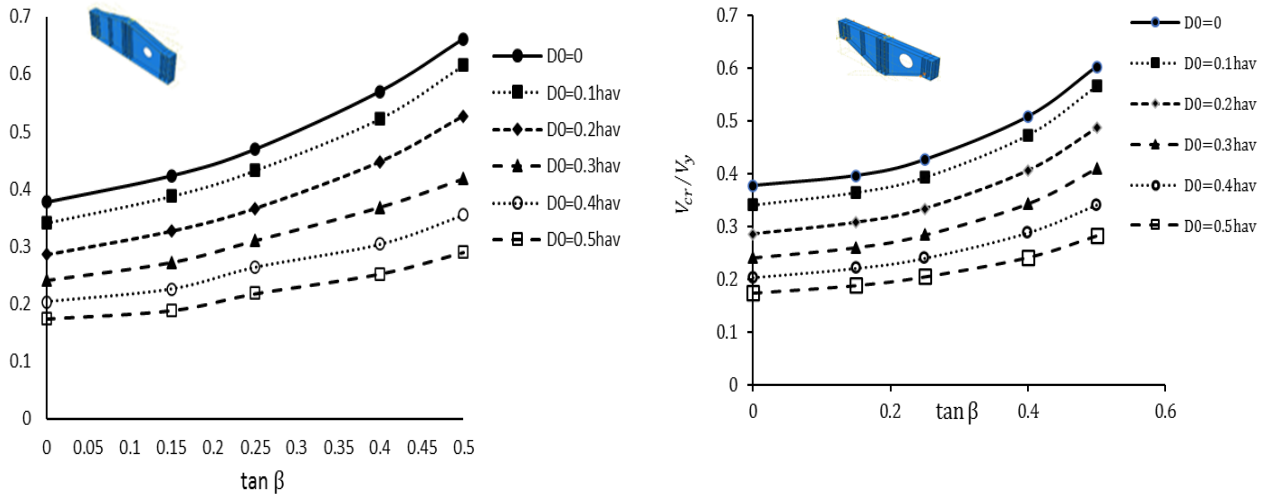

(a)-Typology-I **(b)-Typology-II**

Fig. (10): Effect of tan β on $(\frac{V_{cr}}{V_y})$ with aspect ratio α=1 with different value of circular opening

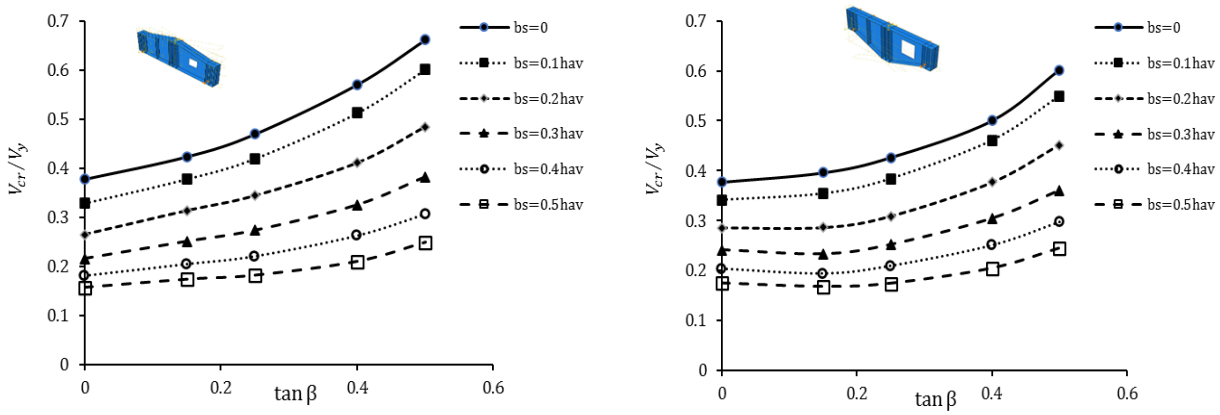

(a)-Typology-I **(b)-Typology-II**

Fig. (11): Effect of (tan β) on $(\frac{V_{cr}}{V_y})$ with aspect ratio α=1 with different value of square opening

5-2 Effect of Type of tapering

As seen above, buckling models of different tapered webs, having the same shape of cut-out, the normalized critical load ($\frac{V_{cr}}{V_y}$) increased with increasing in tapering angle (tan β) On the other hand, the value of the critical shear load decreased with increasing the dimensions of the hole respect to the average height of the web. Fig. (12) illustrates the normalised critical load for two types of typologies and the prismatic web with the same shape opening web and the same aspect ratio. It can be observed from the figure that the normalized critical load ($\frac{V_{cr}}{V_y}$) for the three types is decreased with increasing the dimension of the hole in circular or square shape, while it is higher for Typology I and II than the prismatic web for the same value of size hole.

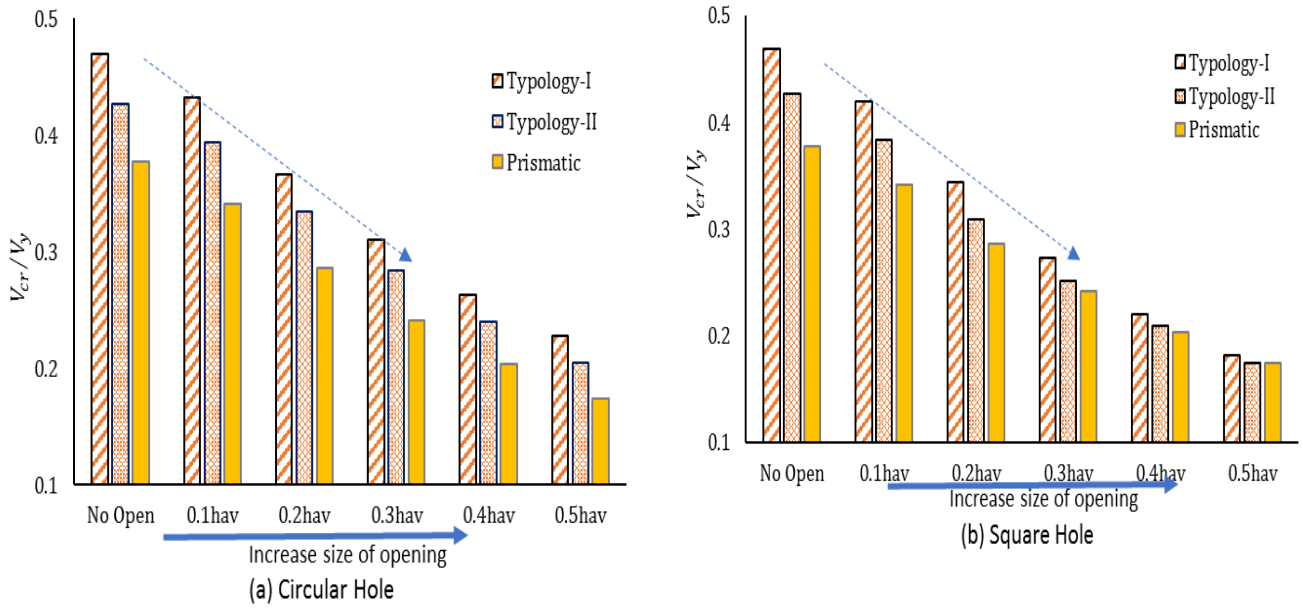

Fig.(12): Normalized critical load for tapered opening webs with aspect ratio (α=1): (a) Circular and (b) Square.

5-3 Assessment of coefficient elastic buckling

Herein, from dissection in section 2, the coefficient elastic buckling because of tapering web, it is obtained from the finite element model is compared with the coefficient elastic buckling calculated by Narayanan and Der Avanessian [8], Lee et al. [30], and Bedynek and Mirambell [23-24], As indicated in Fig. 13(a-b). A regression analysis is conducted on the previous results where a limited coefficient of determination (R^2) value of 0.94 is adopted. Eqs. (12) to (13) show the proposed shear buckling coefficient formulas for tapering web Typology I and II respectively:

$$K_{Tapering-I} = 1.6\tan\beta - \left[(1.72\tan\beta + 0.11)\left(\frac{D_0}{h_{av}}\right)\right] + 0.94 \qquad \text{Typology I} \qquad [12]$$

$$K_{Tapering-II} = 1.3\tan\beta - \left[(1.38\tan\beta + 0.024)\left(\frac{D_0}{h_{av}}\right)\right] + 0.90 \qquad \text{Typology II} \qquad [13]$$

5-4 Comparisons with available coefficient of elastic buckling stresses

5-4-1 Comparison with Narayanan and Der Avanessian [8]

In this section, the critical shear coefficients for prismatic webs (k_{FE}) are compared with the available critical shear stress coefficients proposed by Narayanan and Der Avanessian [8] given in Eq. [5 and 6]. The results of the comparison are provided in Fig. (13). From the comparative results, it can be noticed that in prismatic web the coefficient of critical shear buckling closed with (K_0) the coefficient suggested Eq. [5 and 6] by Narayanan and Der Avanessian [8] with values of dimensions of holes (D_0 or b_s) respect to average height, as shown in Fig. (13-a). On the contrary, the results of comparison from the tapered web containing circular open with tapering angle (tan β=0.25) the results are not closed at small value of ($\frac{D_0}{h_{av}}$) but good result at the value of (D0=0.4hav and 0.5hav) as shown in Fig.(13-b).

5-4-2 Comparison with Bedynek et al. [23-24]

As indicated in Fig. (13-a and b) the coefficient of critical shear of the tapered webs with opening (k_{FE}) are compared with the available coefficient of critical shear stresses suggested by Bedynek et al. [23-24] for Typology-I and II, which was presented in Eq. [14 and 15]:

$$K_{\beta,\alpha} = 5.5\alpha^{0.8}\tan(\beta) + 8.7\alpha^{-0.4} \quad \text{Typology I} \quad [14]$$

$$K_{\beta,\alpha} = 10.6\,\alpha^{0.5}\tan(\beta) + 8.0\,\alpha^{-0.4} \quad \text{Typology II} \quad [15]$$

As can be seen from Fig. (13-a and b), the coefficient of Bedynek et al. [23-24], which utilize only the effect of tapering angle and aspect ratio in calculating the coefficient of shear buckling strength, is not suitable to be used in the prediction equations of coefficient the shear buckling stresses of the tapered opening webs.

5-4-3 Comparison with Lee and Yoo [30]

In this section, the effect of the solid web-to-flange connection is considered since the boundary conditions between the web and the flange of the prismatic cross member are considered important to its behavior. The elastic shear buckling stress coefficients in the web of a rectangular plate girder, including the openings proposed by Narayanan and Der Avanessian [8], as shown in Fig. (13), they assumed that the higher stiffness of the flanges compared to that of the perforated web, the web panels above and below the openings may be assumed clamped along the longitudinal and transverse edges, As given in Equations.[4] to [10] and those proposed by Lee and Yoo [30]. the calculation of the coefficient (k) takes into account the flange constraint is the web rotation. On contrary, Bedynek et al. [23-24] assume that the boundary conditions between the web and flange are simply supported.

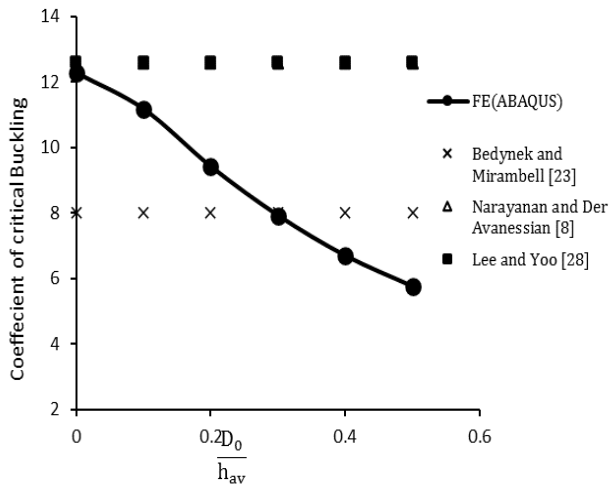

(a)- tan β=0

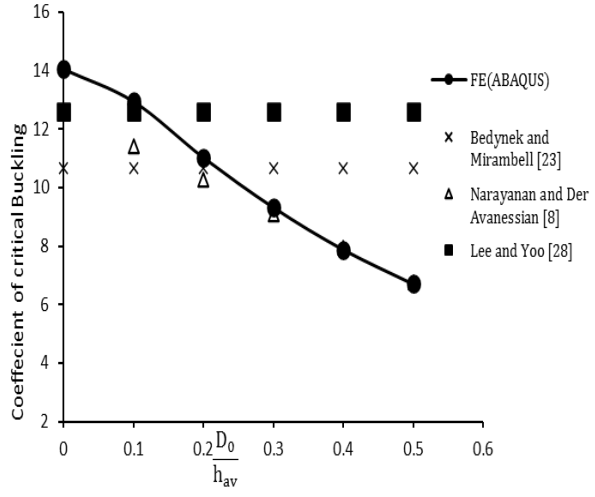

(a)- tan β=0.25

Fig. (13): Comparing the coefficient of critical shear buckling for circular holes at (a) tan β=0 and (b) tan β=0.25

5-5 Estimation of the elastic buckling equations

The parametric analysis results show that the elastic shear stress coefficient of the prismatic and tapered web panels containing holes are governed by end web panel aspect ratio (α=a/h), dimension of the hole respect to the average height, boundary condition between the web and the flange and tapering angle (tan β). The results of the parametric study were used in linear regression analysis to estimate the equations for the coefficients of critical shear stress for prismatic and tapered end webs. The proposed equations are verified by comparison with the formulas available in the literature.

As shown before in section (2) and section (5-3), the coefficient of elastic shear buckling obtained from FEA is compared with the coefficient calculated by Narayanan and Der Avanessian [8] with respect the fixation of the boundary condition between the flange and web, and Bedynek and Mirambell [23-24], for prismatic web (tan β=0), the normalized critical load obtained from the FE is in good agreement with Narayanan and Der Avanessian [8], but the equation not considering the tapering angle in the Eq. [5 and 6]. So, the proposed coefficient equation ($k_{Taper\&open}$) given by Eq. (11) can be calculated by Eq. [12 and 13] and Eq. [16] and [17], which considering the web opening dimension, tapering ratio, aspect ratio, boundary condition between web and flanges and the tapering typology. Finally, the critical load can be calculated by Eq. [18] as follow:

$$K_{open-Cr} = K\left(1 - \frac{1.5(D_o/h_{av})}{\sqrt{\frac{(h_{w1})^2+a^2}{(h_{av})^2}}}\right) \quad \text{For Circular Opening} \qquad [16]$$

$$K_{open-Sr} = K(1 - 1.25\sqrt{\frac{A_s}{A_w}}) \quad \text{For Square Opening} \qquad [17]$$

$$K = 8.98 + 5.61\left(\frac{h_{w1}}{a}\right)^2 - 1.99\left(\frac{h_{w1}}{a}\right)^3 \quad \text{For } \frac{a}{h_{w1}} \geq 1$$

$$V_{Cr} = h_{av}t_w K_{Taper\&open}\frac{E\pi^2}{12(1-\upsilon^2)}\left(\frac{t_w}{h_{w1}}\right)^2 \qquad [18]$$

Equation (18) will be considered for the evaluation of the elastic shear load.

6 Conclusions

In this study, a parametric investigation was developed in linear fields on tapered plates with one hole, subjected to shear loading. The following parameters were considered as effecting on elastic buckling behaviour of plates with one-hole subjected to shear loading:

(a) Hole size respect to the average depth ($\frac{D_0}{h_{av}}$ and $\frac{b_s}{h_{av}} = 0.1,0.2,0.3,0.4\ and\ 0.5$);

(b) Tapered angle (tan β=0, 0.1,0.15,0.25,0.4 and 0.5).

(c) Type of tapering due to inclination of the top or bottom flange (Typology-I and II).

(d) Hole shape (circular or square) and

(e) Aspect ratio (α=1 and 2).

In the case of tapered plates with circular or square holes, $K_{open-Tapering}$ assumes high values as the tapering angle increases and the hole diameter decreases. Furthermore, the type of tapering has a greater impact on the stress state of the inclined flange and the direction of the tension field. The Resal effect, in which the vertical component of the axial force in the inclined flange may increase

or reduce the shear capacity of the tapered panel, also influences these variations. Furthermore, the critical shear load is larger for typologies I than for typologies II and prismatic web, where the critical shear buckling load increases with flange inclination, but this condition does not happen with typologies II and prismatic web. According to the results of this paper, the following conclusions can be drawn:

1. The present numerical formulation to calculating critical shear loading is straightforward, high assurance is achieved with previous experimental and theoretical results.
2. With the present formula, the effect of all various parameters on the critical buckling coefficient can simply studied.
3. The calculation of the critical shear loading in case of tapered plate containing one opening must considering the direction and the angle of the inclined flange as the first step of calculating the load.

Finally, most of the previous research showed that additional tests should be performed for this type of girder considering the effect of all parameters in calculating the critical and ultimate shear loading.

Appendix A

Illustrative example

In this section, two examples will be provided to explain the application of the critical load calculation proposed in this paper to a tapered plate with a circular hole and a tapered plate girder without opening from experimental work by Bedynek et al. [24]. The First example uses the girder tested by Bedynek et al. [24] (**A_600_800_800_4_180_15**); see Table 3. The thickness of the web is 4 mm. The tapered inclination angle is type I, the inclination angle is tanβ=0.25, and the diameter of the circular hole is 210mm. The elastic modulus and Poisson's ratio are 211.3 GPa and 0.3, respectively. To calculate the value of $V_{Cr,Prop}$, the following procedure should be performed:

1- Calculate the coefficient of critical shear load from Eq. [5], Eq.[7], [9],[14] and [18]

$$K = 8.98 + 5.61\left(\frac{800}{800}\right)^2 - 1.99\left(\frac{800}{800}\right)^3 = 12.6$$

$$K_{open-Cr} = 12.6\left(1 - \frac{1.5\times 0}{\sqrt{\frac{(800)^2+(800)^2}{(700)^2}}}\right) = 12.6$$

$$K_{Tapering-I} = 1.6\tan\beta - \left[(1.72\tan\beta + 0.11)\left(\frac{D_0}{h_{av}}\right)\right] + 0.94 = 1.34$$

$$K_{Tapered\&Open} = K_{Open} \times K_{Tapering} = 12.6\times 1.34 = 16.88$$

$$V_{Cr} = h_{av}t_w K_{Tapered\&open}\frac{E\pi^2}{12(1-\upsilon^2)}\left(\frac{t_w}{h_{w1}}\right)^2 = 700\times 4\times 16.88\times\frac{2.113\times 10^5\times\pi^2}{12(1-0.3^2)}\times\left(\frac{4}{800}\right)^2 = 225.6KN$$

This result from the proposed equation is closed with experimental result by Bedynek et al. [24], which the value from the experimental equal (225KN) see Table 3.

The second example uses the model (I-A-Cr-0.25-0.3hav); see Table 5. The thickness of the web is 4 mm. The tapered inclination angle is type I, the inclination angle is tanβ=0.25, and the diameter of

the circular hole is 210mm. The elastic modulus and Poisson's ratio are 210 GPa and 0.3, respectively. To calculate the value of $V_{Cr,Prop}$, the following procedure should be performed:

1- Calculate the coefficient of critical shear load from Eq.[5], Eq.[7],[9], [14] and [18]

$$K = 8.98 + 5.61\left(\frac{800}{800}\right)^2 - 1.99\left(\frac{800}{800}\right)^3 = 12.6$$

$$K_{open-Cr} = 12.6\left(1 - \frac{1.5\times0.3}{\sqrt{\frac{(800)^2+(800)^2}{(700)^2}}}\right) = 10.43$$

$$K_{Tapering-I} = 1.6\tan\beta - \left[(1.72\tan\beta + 0.11)\left(\frac{D_0}{h_{av}}\right)\right] + 0.94 = 1.18$$

$$K_{Tapered\&Open} = K_{Open} \times K_{Tapering} = 10.43\times1.18 = 12.28$$

$$V_{Cr} = h_{av}t_w K_{Tapered\&open}\frac{E\pi^2}{12(1-\upsilon^2)}\left(\frac{t_w}{h_{w1}}\right)^2 = 700\times4\times12.28\times\frac{2.1\times10^5\times\pi^2}{12(1-0.3^2)}\times\left(\frac{4}{800}\right)^2 = 163.14KN$$

References

[1] T. Hoglund, Strength of thin plate girders with circular or rectangular web holes without web stiffeners, Int. Assoc. Bridge Struct. Eng. (IABSE) Colloq.: Des. Plate girders Ultim. Strength (1971) 353–365.

[2] Narayanan R, Rockey KC. Ultimate load capacity of plate girders with webs containing circular cut-outs. Proc Inst Civ Eng 1981; 71:845–62.

[3] Narayanan R, Der Avanessian NGV. Strength of webs containing circular cut-outs. IABSE Proc 1983; 7:64–83.

[4] Narayanan R, Der Avanessian NGV. Equilibrium solution for predicting the strength of webs with rectangular holes. Proc Inst Civ Eng 1983; 75:265–82.

[5] Narayanan R, Der Avanessian NGV. Design of slender webs containing circular hole. IABSE Proc 1984; 8:72–84.

[6] R. Narayanan, Der Avanessian NGV, "An equilibrium method for assessing the strength of plate girders with reinforced web openings. Proceedings of the Institution of Civil Engineers. 77(2): pp. 107–137, 1984.

[7] Narayanan R, Der Avanessian NGV. Strength of webs with corner openings. Struct Eng 1984;62B:6–11.

[8] Narayanan R, Der Avanessian NGV. Elastic buckling of perforated plates under shear. Thin-Walled Struct 1984; 2:51–73.

[9] Narayanan R, Darwish IYS. Strength of slender webs having non-central holes. Struct Eng 1985;63B:57–62.

[10] Narayanan R, Eniolorunda P. Plate girder webs containing a central hole and subjected to bending and shear. Second regional colloquium stability steel structures; 1986. p. 359–66.

[11] P. Carlo, M. Emanuele, M. Claudio, "Linear and non-linear behaviour of steel plates with circular and rectangular holes under shear loading, Thin Walled Struct. 47 (2009) 607–616.

[12] T.M. Roberts, R.I.M. Al-Amery, Shear strength of composite plate girders with web cut-outs, J. Struct. Eng. ASCE 117 (7) (1991) 1897–1910.

[13] N.E. Shanmugam, V.T. Lian, V. The vendran, Finite element modelling of plate girders with web openings, Thin Walled Struct. 40 (2002) 443–464.

[14] Porter DM, Cherif ZEA. Ultimate shear strength of thin webbed steel and concrete composite girders. In: Narayanan R, editor. Composite steel structures: advances, design, and construction. Routledge; 1987. p. 55–64.

[15] M.Y.M. Yatim, N.E. Shanmugam, W.H. Wan Badaruzzaman, Behaviour of partially connected composite plate girders containing web openings, Thin Walled Struct. 72
(2013) 102–112.

[16] M.J. Hamoodi, M.S. Abdul Gaber, Behavior of steel plate girders with web openings loaded in shear, Eng. Tech. J. (2013) 2982–2996, 31 Part (A), No. 15.
[17] Paik JK. Ultimate strength of perforated steel plates under shear loading. Thin-Walled Structures 2007; 45:301–6.
[18] S.P. Timoshenko, J.M. Gere, Theory of the Elastic Stability, second ed., McGraw Hill Co., Inc., New York (USA), 1961.
[19] N. Hagen, P. Larsen, Shear capacity of steel plate girders with large web openings. Part II: design guidelines, J. Constr. Steel Res. 65 (2009) 151–158.
[20] EN 1993-1-5 Eurocode 3–Design of steel structures–Part 1-5: Plated structural elements. 2006. CEN
[21] M.R. Azmi, M.Y.M. Yatim⁎, A. Esa, W.H. Wan Badaruzzaman. Experimental studies on perforated plate girders with inclined stiffeners, Thin Walled Struct. 117 (2017) 147–256.
[22] Mirambell E, Z´arate AV. Web buckling of tapered plate girders. Proc Inst Civ Eng - Struct Build 2000;140(1):51–60.
[23] Bedynek Agnieszka, Real Esther, Mirambell Enrique. Shear buckling coefficient: proposal for tapered steel plates. Proc Inst Civil Eng - Struct Build 2014;167(4): 243–52.
[24] A. Bedynek, E. Real, and E. Mirambell, "Tapered plate girders under shear: Tests and numerical research," Eng. Struct., vol. 46, pp. 350–358, 2013. https://doi:10.1016/j.engstruct.2012.07.023.
[25] Serror Mohammed H, Abdelbaset Basem H, Sayed Hesham S. Shear strength of tapered end web panels. J Constr Steel Res 2017; 138:513–25.
[26] American Association of State Highway and Transportation Officials, AASHTO LRFD Bridge Design Specifications,2017. https://doi.org/10.1017/ CBO9781107415324.004
[27] Research Centre for Housing and Physical Planning in Cairo. Egyptian Code of Practice for Steel Construction and Bridges. vol. No.451. 2008.
[28] Gendy Bassem L. Critical shear buckling load of tapered plate with circular opening. HBRC J 2016;12(3):296–304.
[29] ABAQUS Standard User's Manual. The Abaqus Software is a product of Dassault Systems Similia Corp., Providence, RI, USA Dassault Systems, Version 6.13, USA; 2013.
[30] Lee SC, Davidson JS, Yoo CH. Shear buckling coefficients of plate girder web panels. Comput Struct 1996;59(5):789–95.

دراسة الانبعاج المرن للكمرات المعدنيه ذات الاعصاب المنشوريه وتحتوي على فتحات

الملخص باللغة العربية:

تعتبر الكمرات المنشورية هي الأفضل في تصميم المباني الصناعية والكباري ذات البحور الكبيرة. واحتواء هذه الكمرات على فتحات في أعصاب الكمرات لتوفير مساحة للخدمات وتقليل التكاليف الخاصة بالتصنيع. لذا كان من الضرورى دراسة هذا النوع من الكمرات وهو الهدف الذي تم من خلاله اعداد هذه الورقة البحثية لدراسة وتقدير قيمة الاحمال الحرجة تحت تأثير قوى القص لكمرات منشوريه وكذلك تحتوي على فتحات مربعه ومستديره. حيث تمت الدراسة باستخدام برامج العناصر المحدده على عدد ١٧٦ كمره لكمرات منشوريه وتحتوي على نوعين من الفتحات (دائرية ومربعه) حيث الاخذ في الاعتبار دراسة تأثير اختلاف الأعماق وابعاد هذه الفتحات وكذلك مساحة هذه الفتحات للعمق المتوسط للويب ونسبة العرض الى الارتفاع ونسبة العمق الى سماكة الاعصاب. ومن خلال دراسة نتائج هذا التحليل العددى تم استنتاج معادلة لتقدير قيمة الحمل الحرج لقوى القص لكلا النوعين من الكمرات المستقيمة والمنشوريه والتي تحتوي على فتحات مختلفة الشكل سواء دائريه او مربعة